Laser additive manufacturing of graphene/CoCrFeNiNbx coatings and their application in automatic measurement robot devices

Chunge Liu[1], Xingwu Qiu[1]*, Zhansheng Wang[1], Biao Zhong[1], Jia Peng[1],
Zhongwei Liu[1], Hong Liu[1], Yan Gao[1], Haoqiang Wu[1], Xuan Zhou[1], Chengquan Luo[1],
Xinran Xie[1], Chao Meng[2]

[1]*Sichuan College of Architectural Technology, Deyang 618000, P. R. China*
[2]*Liaoning Technical University, Fuxin 123000, P. R. China*

Abstract

The stabilizing device is a component of the automatic surveying robot. To address wear and tear on the friction plates during use, graphene (Gr)/high-entropy alloy coatings were applied to the aluminum alloy friction plates using laser cladding technology. A systematic study was conducted on the alloy using scanning electron microscopy/EDS, a hardness tester, a friction and wear tester, etc. The experimental results show that the coating bonds well to the substrate. The Gr/CoCrFeNiNbx coating is mainly composed of equiaxed crystals, with Gr playing a strengthening role and Nb element playing a fine grain strengthening role. The coating has excellent mechanical properties, with a microhardness between 462–487 HV and an average friction coefficient between 0.46–0.54. Through practice, laser cladding a Gr/CoCrFeNiNbx coating on the surface of the stable device of the automatic surveying robot ensures its normal operation and extends its service life.

K e y w o r d s: laser additive manufacturing, coating, robot device, automatic surveying, high entropy alloy, wear resistance

1. Introduction

High entropy alloys have attracted widespread attention due to their excellent mechanical properties [1–8], corrosion resistance [9–16], and high-temperature performance [17–20]. In particular, laser cladding technology for preparing high-entropy alloy coatings has played a key role in component repair, surface modification, and other applications [21–24]. Due to the adjustable thickness of the coating produced by laser cladding, it exhibits metallurgical bonding with the substrate and a small heat-affected zone, thereby significantly improving the performance and service life of components.

The stabilizing device is a component of the automatic surveying robot [25–28], which is equipped with friction plates. To meet lightweight requirements, the friction plates are made of aluminum alloy, and the vertical rotation device is stabilized by friction between the friction plates and the wheel axle.

The actual effect verification of the robot device based on automatic surveying showed that the friction plate of the stabilizing device is prone to wear during use, leading to a loss of fixing effect and affecting surveying. To solve this problem, this study prepared Gr/high-entropy alloy coatings on the surfaces of aluminum alloy friction plates via laser cladding to improve friction performance.

2. Experimental

Powdered cobalt, chromium, iron, nickel, niobium elements, and Gr were selected as laser cladding powders; the purity of the metal powder is not less than 99.9 %, and the purity of Gr is not less than 99 %. The powder particle size range used is 45–150 μm. Particle size distribution: particles ≤ 45 μm should not exceed 5 %, and particles > 150 μm should not exceed 5 %. In order to prepare Gr/CoCrFeNiNb composite powder,

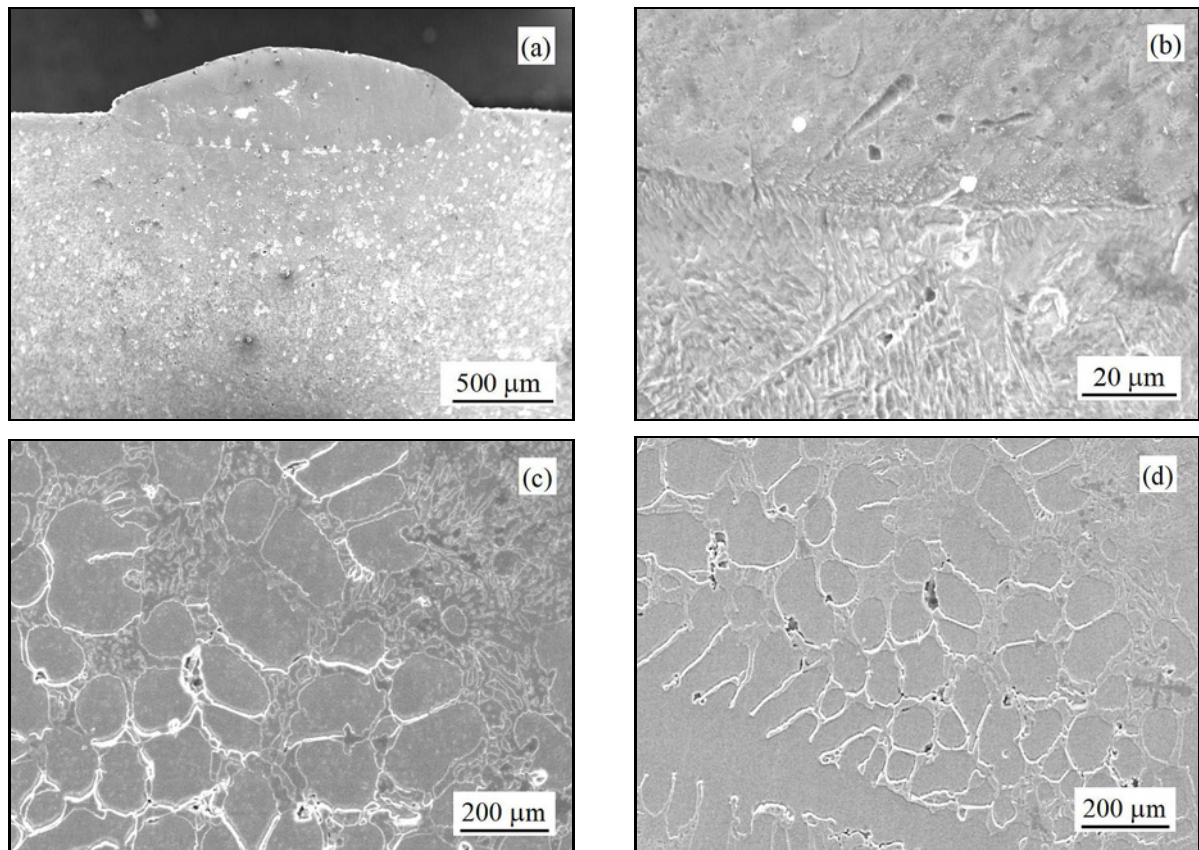*Corresponding author: e-mail address: qiuxingwu2021@163.com

Fig. 1. Morphology of laser cladding coatings: (a) macroscopic morphology, (b) bonding area between the cladding coating and the substrate, (c) microstructure of Gr/CoCrFeNiNb0.15, and (d) microstructure of Gr/CoCrFeNiNb0.30.

0.30 wt.% Gr was added to the CoCrFeNiNbx (x = 0.15, 0.3) powder. The mixed powder was ball milled in a planetary mill for 4 hours at a rotational speed of $300\,\mathrm{r\,min^{-1}}$. During ball milling of high entropy alloy powder for laser cladding, a ball-to-powder ratio of $10:1$ was used. To improve efficiency and reduce energy consumption, three sizes of grinding balls (20, 10, and 6 mm) were used in a multi-stage ball configuration with a ratio of $3:5:2$. Appropriate ball milling time (e.g., 4–8 hours) can enhance the uniformity of element distribution; however, excessive milling may lead to flaky morphology and welding, reducing uniformity. The obtained powder particles are mainly distributed between 10 and 150 μm. Milling time affects the phase structure; for example, in the CoCrMoNbTi system [29], as milling time increases, the diffraction peaks of the pure elements disappear in order of their melting points. After 40 hours of milling, a single--phase body-centered cubic solid solution can form, but excessive milling may lead to phase decomposition or the formation of non-equilibrium phases. The obtained powder needs to be filtered and classified using a 75 μm sieve to control the particle size distribution. Aluminum alloy is used as the substrate material for the friction plate of the automatic surveying robot. Ground aluminum alloy substrates remove surface oil

stains, ensuring cleanliness. This complete set of CO_2 laser cladding equipment uses a CO_2 laser (TFL-6K) as the heat source and includes a laser, a dedicated cooling unit, a CNC machining machine, an automatic powder feeder, an optical system, and CNC software. The laser processing parameters were laser power $P = 2000\,\mathrm{W}$, scanning speed $V = 6\,\mathrm{mm\,s^{-1}}$, and laser spot diameter $D = 4.0\,\mathrm{mm}$.

The microstructure of Gr/CoCrFeNiTi HEAs was observed by scanning electron microscope (KYKY--EM3200). The HVS-1000Z microhardness tester was used to test the hardness of Gr-reinforced HEAs. The friction and wear performance of Gr-reinforced HEAs was tested using the SFT-2M pin disc friction and wear testing machine, with a loading of 15 N and a testing time of 900 s.

3. Results and discussion

3.1. Microstructure

Figure 1a shows the macroscopic morphology of the laser cladding layer, where a strong bonding between the coating and the substrate is observed. Under the action of a high-energy laser beam, the cladding
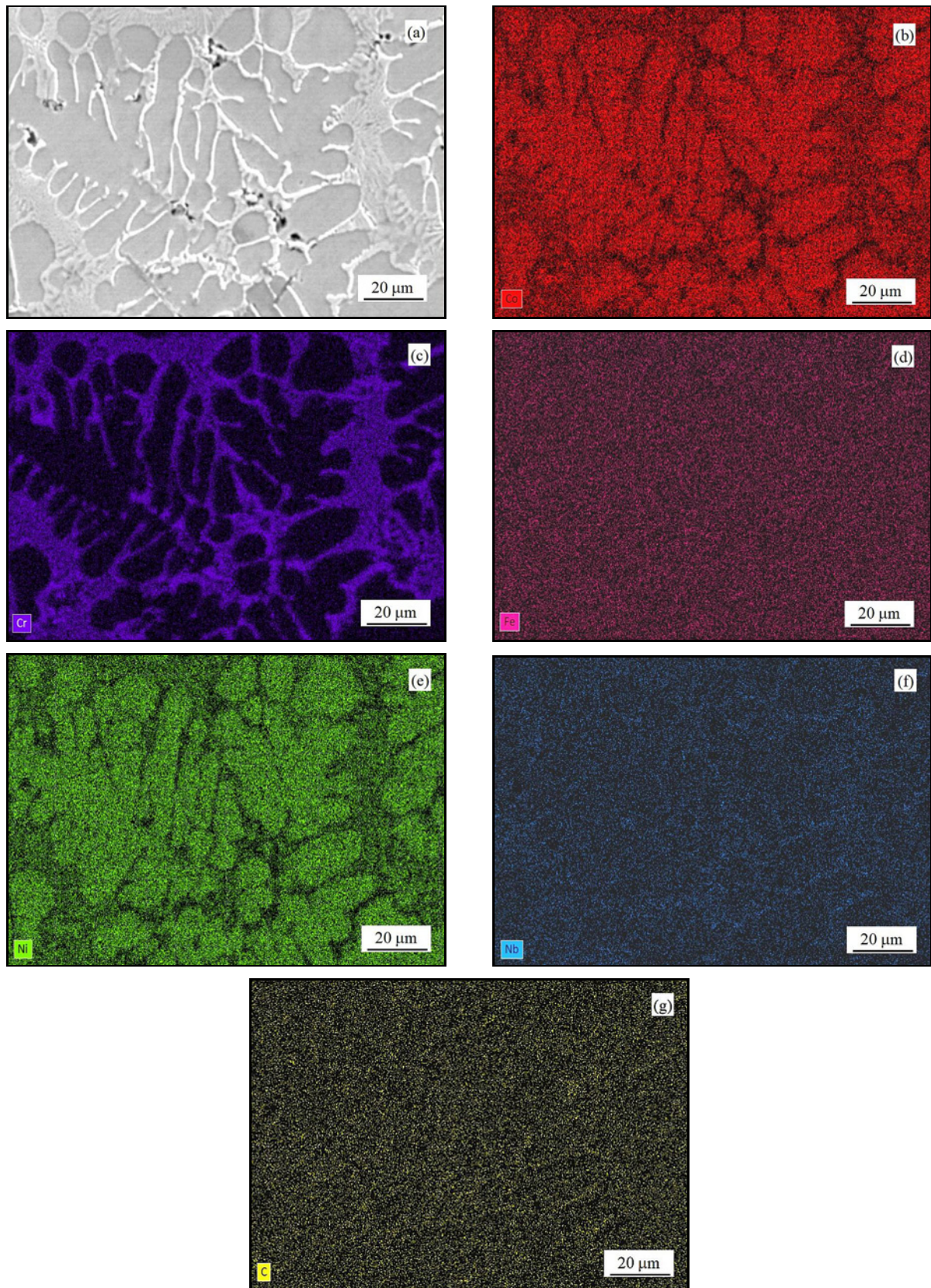
Fig. 2. Elemental surface scanning of Gr/CoCrFeNiNb0.30 coatings.

powder melts, while the substrate also forms a thin molten layer due to thermal effects. Subsequently, the liquid metal solidifies under the cooling influence of the substrate, forming the laser-cladding layer. Fig-

ure 1b presents an enlarged view of the bonding interface between the cladding coating and the substrate. The interface exhibits an arc-like shape, with the highest temperature corresponding to the center of the laser beam, resulting in the deepest surface melting of the substrate. Near the edges of the beam, the temperature is lower, leading to shallower surface melting of the substrate, thus forming this arc-shaped pattern. This also indicates a favorable metallurgical bond between the coating and the substrate, ensuring the coating's superior performance. Figures 1c,d show the microstructure of Gr/CoCrFeNiNbx coatings, mainly composed of fine equiaxed grains and precipitates. The small microstructure size is due to the rapid heating and cooling of the laser cladding process. Under the action of high-energy laser beams, the powder and the aluminum alloy surface are instantly melted to form a molten pool, with many crystal nuclei in its center. Under the rapid cooling of the aluminum alloy, the grains do not have time to grow, resulting in a fine equiaxed microstructure. On the other hand, the addition of Gr refines the grain size, and the increase in Nb content further refines the alloy structure, thereby refining the grain size [30, 31]. The coating has a small number of pores, and the porosity is approximately 1 % as calculated. There have been precipitates in the microstructure. During rapid solidification of high-entropy alloys by laser cladding, the diffusion rates of various elements differ, leading to supersaturation of the solid solution, segregation of solute atoms at grain boundaries and within grains, and the formation of precipitates. Precipitates significantly influence the microstructure and properties by refining grain size and precipitate strengthening: they hinder dislocation motion and grain boundary sliding, thereby enhancing strength, hardness, and toughness, while also optimizing the microstructure to improve wear resistance.

Nb can refine grain size and promote the formation of a layered eutectic structure. Gr has excellent physical and chemical properties that promote carbide formation, further refine grains, and improve tissue uniformity. The precipitate can refine grain size, reduce grain-boundary defects, and make the structure more uniform and denser.

Elemental surface scanning was performed, and the results are shown in Fig. 2. The results indicate that the coating consists of two phases: face-centered cubic (FCC) and body-centered cubic (BCC). Equiaxed grains (FCC) mainly contain Co and Ni elements, while grain boundaries and precipitates (BCC) mainly contain Cr elements. The distribution of other elements is relatively uniform.

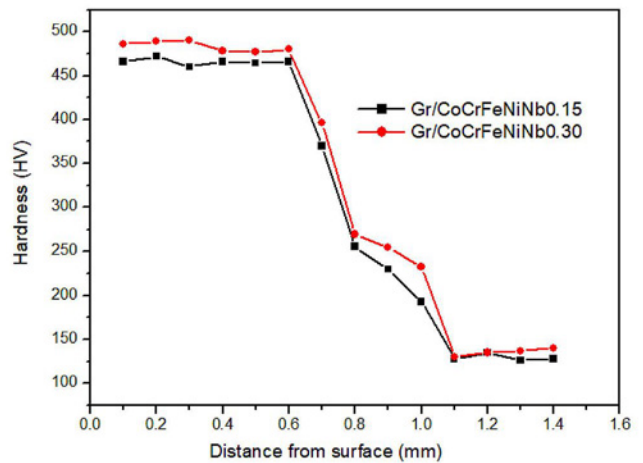### 3.2. Hardness

Figure 3 shows the hardness distribution curves for
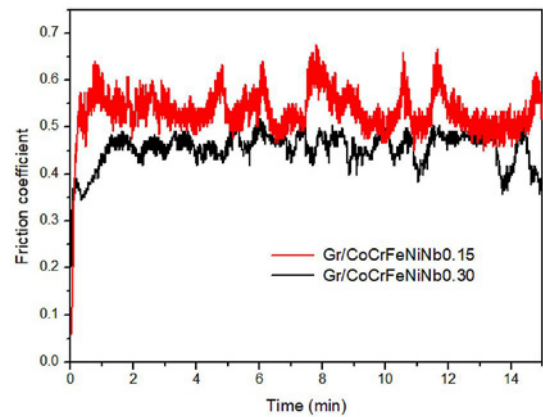
Fig. 3. Microhardness of Gr/CoCrFeNiNbx coatings.

Fig. 4. Wear morphology of Gr/CoCrFeNiNbx alloys.

Gr/CoCrFeNiNbx alloys, divided into three regions: coating, heat-affected zone, and substrate. The significant increase in coating hardness is mainly due to the strengthening effect of Gr and the fine-grain strengthening effect of Nb. Nb and C (derived from Gr) generate stable carbides, refine grain size, and achieve dispersion strengthening, which can significantly improve the hardness of the alloy. Precipitation strengthening also contributes to improving the hardness of alloys.

3.3. Wear resistance

Figure 4 shows the friction coefficient curves of Gr/CoCrFeNiNbx coatings. The average friction coefficient of the Gr/CoCrFeNiNb0.15 coating is 0.54, and the average friction coefficient of the Gr/CoCrFeNiNb0.30 coating is 0.46. The low friction coefficient of the coatings indicates that the alloys exhibit excellent wear resistance, which is related to their
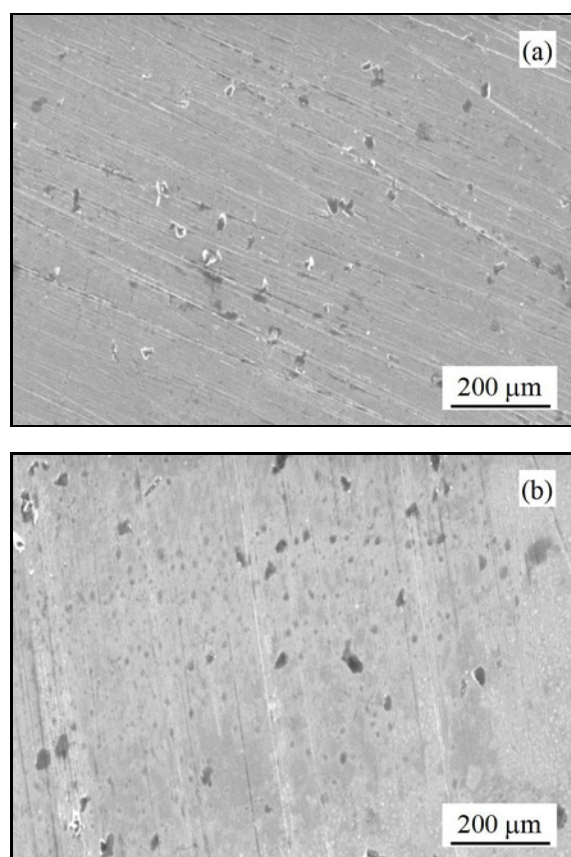
Fig. 5. Friction coefficient curve of Gr/CoCrFeNiNbx coatings: (a) Gr/CoCrFeNiNb0.15 and (b) Gr/CoCrFeNiNb 0.30.

hardness and ductility. The combination of hardness and ductility ensures the wear resistance of the alloy [32, 33]. Nb can improve the wear resistance of coatings through solid solution strengthening and precipitation strengthening. Gr can form a stable lubricating film, disperse contact stress, and suppress dislocation activity, effectively reducing the friction coefficient. The precipitation improves the microstructure and reduces wear by increasing hardness.

Figure 5 shows the wear morphology of the coatings, with shallow adhesive wear pits and shallow abrasive wear plowing grooves on the alloy surface. The wear mechanism is a mixture of adhesive wear and abrasive wear. Gr has good self-lubricating properties and acts as a lubricant between the friction pair and the substrate. After being subjected to the friction-induced stress, the debris scratches the surface of the abrasion and forms plowing grooves. Compared with the wear morphology of Gr/CoCrFeNiNb0.15 and Gr/CoCrFeNiNb0.30 alloys, the wear morphology of Gr/CoCrFeNiNb0.30 alloy is milder, mainly due to the strengthening effect of the Nb element.

4. Conclusions

(i) Laser cladding of Gr/CoCrFeNiNbx coatings was applied to the surface of the stabilizing device of the automatic surveying robot. The coating exhibits strong adhesion to the substrate, and its microstructure is primarily composed of equiaxed crystals.

(ii) Gr plays a strengthening role in the alloy, while the Nb element plays a role in fine-grain strengthening.

(iii) The coatings have excellent mechanical properties, with a microhardness between 462–487 HV and an average friction coefficient between 0.46–0.54.

(iv) By laser cladding Gr/CoCrFeNiNbx coating on the surface of the stabilizing device of the automatic surveying robot, it can ensure the normal operation of the surveying robot and extend its service life.

References

[1] Y. H. Wang, Y. Yuan, J. B. Yu, H. H. Wu, Z. P. Lu, Design for thermal stability of nanocrystalline alloys based on high-entropy effects, Acta Metall. Sin. 57 (2021) 403–412. (in Chinese)
https://doi.org/10.11900/0412.1961.2020.00494

[2] H. Torres, S. Slawik, C. Gachot, B. Prakash, M. R. Ripoll, Microstructural design of self-lubricating laser claddings for use in high temperature sliding applications, Surf. Coat. Tech. 337 (2018) 24–34.
https://doi.org/10.1016/j.surfcoat.2017.12.060

[3] Y. Zhang, Z. Chen, D. D. Cao, J. Y. Zhang, P. Zhang, Q. Tao, X. Q. Yang, Concurrence of spinodal decomposition and nano-phase precipitation in a multi-component AlCoCrCuFeNi high-entropy alloy, J. Mater. Res. Technol. 8 (2019) 726–736.
https://doi.org/10.1016/j.jmrt.2018.04.020

[4] C. B. Guo, Y. B. Lian, C. Huang, Z. Y. Chen, pH-responsive capsule loaded with nitrogen-doped carbon dots for metal corrosion protection, J. Mater. Res. Technol. 25 (2023) 2306–2323.
https://doi.org/10.1016/j.jmrt.2023.05.283

[5] Y. Z. Shi, B. Yang, X. Xie, J. Brechtl, K. A. Dahmen, P. K. Liaw, Corrosion of Al$_x$CoCrFeNi high-entropy alloys: Al-content and potential scan-rate dependent pitting behavior, Corros. Sci. 119 (2017) 33–45. https://doi.org/10.1016/j.corsci.2017.02.019

[6] S. Xiang, H. Luan, J. Wu, K. F. Yao, L. Qiang, Microstructures and mechanical properties of CrMnFeCoNi high entropy alloys fabricated using laser metal deposition technique, J. Alloy. Compd. 773 (2019)

387–392.
https://doi.org/10.1016/j.jallcom.2018.09.235

[7] S. J. Sun, Y. Z. Tian, H. R. Lin, X. G. Dong, Y. H. Wang, Z. J. Zhang, Z. F. Zhang, Enhanced strength and ductility of bulk CoCrFeMnNi high entropy alloy having fully recrystallized ultrafine-grained structure, Mater. Design 133 (2017) 122–127.
https://doi.org/10.1016/j.matdes.2017.07.054

[8] M. Song, R. Zhou, J. Gu, Z. W. Wang, S. Ni, Y. Liu, Nitrogen induced heterogeneous structures overcome strength-ductility trade-off in an additively manufactured high-entropy alloy, Appl. Mater. Today 18 (2020) 100498.
https://doi.org/10.1016/j.apmt.2019.100498

[9] S. S. Nene, S. Sinha, M. Frank, K. Liu, R. S. Mishra, B. A. McWilliams, K. C. Cho, Unexpected strength-ductility response in an annealed, metastable, high-entropy alloy, Appl. Mater. Today 13 (2018) 198–206.
https://doi.org/10.1016/j.apmt.2018.09.002

[10] G. A. Salishchev, M. A. Tikhonovsky, D. G. Shaysultanov, N. D. Stepanov, A. V. Kuznetsov, I. V. Kolodiy, A. S. Tortika, O. N. Senkov, Effect of Mn and V on structure and mechanical properties of high-entropy alloys based on CoCrFeNi system, J. Alloy. Compd. 591 (2014) 11–21.
https://doi.org/10.1016/j.jallcom.2013.12.210

[11] L. Liu, J. B. Zhu, C. Zhang, J. C. Li, Q. Jiang, Microstructure and the properties of FeCoCuNiSn$_x$ high entropy alloys, Mat. Sci. Eng. A 548 (2012) 64–68.
https://doi.org/10.1016/j.msea.2012.03.080

[12] Z. M. Li, K. G. Pradeep, Y. Deng, D. Raabe, C. C. Tasan, Metastable high-entropy dual-phase alloys overcome the strength–ductility trade-off, Nature 534 (2016) 227–230.
https://doi.org/10.1038/nature17981

[13] Z. H. He, Y. C. Dong, Y. Tian, Y. X. Wang, D. S. Zhao, X. Yang, Y. Yang, H. J. Zhao, Effect of Cr content on the microstructure and corrosion resistance of laser cladded FeCoNiMnAl$_{0.5}$Cr$_x$ high entropy alloy coatings, J. Alloy. Compd. 1043 (2025) 184249.
https://doi.org/10.1016/j.jallcom.2025.184249

[14] Q. Q. Cheng, J. L. Chen, G. W. Yi, Y. Shan, Y. S. Geng, J. Y. Wang, W. Z. Wang, Comparative study of the microstructure and phase evolution of FeCoCr-NiAl high-entropy alloy-matrix WC nanocomposite powders prepared by mechanical alloying, J. Alloy. Compd. 938 (2023) 168518.
https://doi.org/10.1016/j.jallcom.2022.168518

[15] X. W. Qiu, C. G. Liu, J. Peng, Z. S. Wang, Corrosion behavior of CoCrNiAl high entropy alloy and other typical metals in simulated acid rain solution, Kovove Mater. 61 (2023) 59–67.
https://doi.org/10.31577/km.2023.1.59

[16] F. B. Kuang, H. Hou, C. H. Yin, J. Z. Wu, Y. C. Ruan, P. F. Liu, The influences of Mo content on the tribological and corrosion properties of FeCrNiSi$_{0.5}$Mo$_x$ high-entropy alloy coatings, J. Alloy. Compd. 1041 (2025) 183696.
https://doi.org/10.1016/j.jallcom.2025.183696

[17] X. L. Di, H. Z. Xu, C. Wang, Y. J. Zhou, S. Y. Peng, X. B. Wang, C. M. Liu, Y. L. Guo, High-temperature dynamic mechanical properties of V$_{0.5}$Nb$_{0.5}$ZrTi refractory high entropy alloy fabricated by multi-wire arc additive manufacturing, Int. J. Refract. Met. H.

134 (2026) 107506.
https://doi.org/10.1016/j.ijrmhm.2025.107506

[18] Y. H. Zhou, J. Y. Zhang, J. Zhang, X. Y. Yao, J. H. Luan, Q. Li, S. F. Liu, B. Xiao, J. Ju, S. J. Zhao, Y. L. Zhao, Z. Y. Sun, H. Nan, M. Yan, T. Yang, A strong-yet-ductile high-entropy alloy in a broad temperature range from cryogenic to elevated temperatures, Acta Mater. 268 (2024) 119770.
https://doi.org/10.1016/j.actamat.2024.119770

[19] M. M. Fang, X. Y. Yue, Y. T. Dong, Y. M. Chen, Z. Liang, A temperature-dependent solvating electrolyte for wide-temperature and fast-charging lithium metal batteries, Joule 8 (20241) 91–103.
https://doi.org/10.1016/j.joule.2023.12.012

[20] X. H. Cao, Y. T. Gao, Z. H. Wang, H. Z. Zeng, Y. F. Song, S. G. Tang, L. Luo, S Gong, FeNiCrCoMn high-entropy alloy nanoparticles loaded on carbon nanotubes as bifunctional oxygen catalysts for rechargeable zinc-air batteries, ACS Appl. Mater. Interfaces 15 (2023) 32365–32375.
https://doi.org/10.1021/acsami.3c04120

[21] W. M. Guo, N. Ding, G. Q. Liu, C. N. Jing, H. X. Xu, L. Liu, N. Xu, X. F. Wu, J. Q. He, F. Zaïri, Microstructure evolution of a multi-track Al-CoCrFeNi high entropy alloy coating fabricated by laser cladding, Mater. Charact. 184 (2022) 111660.
https://doi.org/10.1016/j.matchar.2021.111660

[22] X. F. Li, Y. H. Feng, B. Liu, D. H. Yi, X. H. Yang, W. D. Zhang, G. Chen, Y. Liu, P. K. Bai, Influence of NbC particles on microstructure and mechanical properties of AlCoCrFeNi high-entropy alloy coatings prepared by laser cladding, J. Alloy. Compd. 788 (2019) 485–494.   https://doi.org/10.1016/j.jallcom.2019.02.223

[23] K. Huang, L. Chen, X. Lin, H. S. Huang, S. H. Tang, F. L. Du, Wear and corrosion resistance of Al$_{0.5}$CoCrCuFeNi high entropy alloy coating deposited on AZ91D magnesium alloy by laser cladding, Entropy 20 (2018) 915.
https://doi.org/10.3390/e20120915

[24] X. W. Qiu, M. J. Wu, C. G. Liu, Y. P. Zhang, C. X. Huang, Corrosion performance of Al$_2$CrFeCo$_x$CuNiTi high-entropy alloy coatings in acid liquids, J. Alloy. Compd. 708 (2017) 353–357.
https://doi.org/10.1016/j.jallcom.2017.03.054

[25] G. Bayar, M. Bergerman, A. B. Koku, E. I. Konukseven, Localization and control of an autonomous orchard vehicle, Comput. Electron. Agric. 115 (2015) 118–128.
https://doi.org/10.1016/j.compag.2015.05.015

[26] H. Zhang, Y. Song, C. Han, L. Zhang, Remote sensing image spatiotemporal fusion using a generative adversarial network, IEEE Trans. Geosci. Remote Sens. 59 (2020) 4273–4286.
https://doi.org/10.1109/TGRS.2020.3010530

[27] T. Bak, H. Jakobsen, Agricultural robotic platform with four wheel steering for weed detection, Biosyst. Eng. 87 (2) (2004) 125–136.
https://doi.org/10.1016/j.biosystemseng.2003.10.009

[28] R. Manish, Y. C. Lin, R. Ravi, S. M. Hasheminasab, T. Zhou, A. Habib, Development of a miniaturized mobile mapping system for in-row, under-canopy phenotyping, Remote Sens. 13 (2021) 276.
https://doi.org/10.3390/rs13020276

[29] X. L. Zhou, L. J. He, M. N. Zhang, P. Wang, Effect of ceramic particles on microstructure and properties of CoCrMoNbTi high-entropy alloy coating fabricated by laser cladding, Optik 285 (2023) 170987. https://doi.org/10.1016/j.ijleo.2023.170987

[30] E. H. Wang, J. Q. Li, F. W. Kang, F. C. Jiang, L. S. Lv, B. Dai, Y. Cao, W. Jiang, Balancing the mechanical properties of $Al_{0.45}CoCrFeNiTi_x$ high-entropy alloys by tailoring titanium content, J. Mater. Res. Technol. 28 (2024) 967–979. https://doi.org/10.1016/j.jmrt.2023.12.079

[31] J. W. Yeh, Alloy design strategies and future trends in high-entropy alloys, JOM 65 (2013) 1759–1771. https://doi.org/10.1007/s11837-013-0761-6

[32] X. W. Qiu, Y. P. Zhang, L. He, C. G. Liu, Microstructure and corrosion resistance of AlCrFeCuCo high-entropy alloy, J. Alloy. Compd. 549 (2013) 195–199. https://doi.org/10.1016/j.jallcom.2012.09.091

[33] D. B. Miracle, O. N. Senkov, A critical review of high entropy alloys and related concepts, Acta Mater. 122 (2016) 488–511. https://doi.org/10.1016/j.actamat.2016.08.081